Dictyostelium discoideum Myosin II: Characterization of Functional Myosin Motor Fragments†

S. E. Kurzawa,‡ D. J. Manstein,§ and M. A. Geeves*,‡

Max-Planck-Institut für Molekulare Physiologie, Rheinlanddamm 201, 44139 Dortmund, Germany, Max-Planck-Institut für Medizinische Forschung, Jahnstrasse 29, 69120 Heidelberg, Germany, and National Institute for Medical Research, The Ridgeway, Mill Hill, London NW7 1AA, U.K.

Received August 27, 1996; Revised Manuscript Received November 4, 1996⊗

ABSTRACT: The transient kinetic properties of the recombinant myosin head fragments M761 and M781, which both lack the light chain binding domain (LCBD) and correspond to the first 761 and 781 residues of *Dictyostelium discoideum* myosin II, were compared with those of the subfragment 1-like fragment M864 and a shorter catalytic domain fragment M754. The properties of M761, M781, and M864 are almost identical in regard to nucleotide binding, nucleotide hydrolysis, actin binding, and the interactions between actin and nucleotide binding sites. Only the rate of the hydrolysis step was significantly faster for M761 and the affinity of M781 for actin significantly weaker than for M864. This indicates that the LCBD plays no major role in the biochemical behavior of the myosin head. In contrast, loss of the peptide between 754 and 761 produced several major changes in the property of M754 as documented previously [Woodward, S. K. A., Geeves, M. A., & Manstein, D. J. (1995) *Biochemistry 34*, 16056−16064]. We further show that C-terminal extension of M761 with one or two α-actinin repeats has very little effect on the behavior of the protein. The recombinant nature of M761 and the fact that it can be produced and purified in large amounts make it an ideal construct for systematic studies of the structure, kinetics, and function of the myosin motor.

The myosin head, frequently referred to as subfragment 1 (S1),[1] consists of an N-terminal globular domain from which a long α-helix emerges that is complexed by the essential (ELC) and regulatory (RLC) light chains. The globular domain contains the binding sites for both actin and nucleotide and is hence referred to as the catalytic domain. The complex formed by the long α-helix and the light chains is known as the light chain binding domain (LCBD) or regulatory domain. Recent studies, using both recombinant and proteolytic myosin head fragments (MHF), have shown conclusively that the LCBD is not an essential part of the myosin motor (Itakura et al., 1993; Waller et al., 1995; Uyeda et al., 1996). However, it remains controversial whether removal of the LCBD can be achieved without affecting the kinetic properties of the motor (Woodward et al., 1995). The changes in kinetics properties that were observed with several motor domain fragments could stem from either a requirement for the presence of the LCBD or from a local structural disturbance at the site of truncation. Evidence that the latter might be the case came from work on a proteolytic fragment that extended 13 amino acids into the LCBD but could no longer bind a light chain (Waller et al., 1995) and a recombinant *Dictyostelium discoideum* myosin II that completely lacks the LCBD (Uyeda et al., 1996). These fragments translocate actin filaments in an *in vitro* motility assay and display normal steady-state kinetics.

Our goal was to identify a MHF that displays normal kinetics and good motility behavior and can be produced in large quantities for structural studies. The eukaryotic organism *D. discoideum* has proven to be a very powerful system for the expression and characterization of recombinant myosins, and a number of expression vectors and efficient purification protocols were developed for the production of myosin motors in this host (Manstein et al., 1995a). A number of MHFs were produced using this system. The molecules described here are derived from *D. discoideum* myosin II and are truncated at sites varying from the position where the long α-helix emerges from the catalytic domain to a site that corresponds to residue 15 of the first IQ repeat of the LCBD (Figure 1, Table 1). In order to create molecular motors with motility properties similar to those of a native myosin but which only consist of a single polypeptide chain, several of the MHFs were fused to one or two α-actinin repeats. Each α-actinin repeat is predicted to form a 6 nm left-handed coiled coil formed by three antiparallel α-helices (Cohen & Parry, 1994; Yan et al., 1993). The resulting structure is expected to resemble the LCBD in rigidity and stiffness. Here we present data for constructs comprising the first 761 (M761) and 781 (M781) amino acids of *D. discoideum* myosin II and compare them with data obtained in our previous studies of M754 (Woodward et al., 1995) and the S1-like fragment M864 (Ritchie et al., 1993). Additionally, the data are complemented by those obtained with M754 and M761 constructs fused to one or two α-actinin repeats (Anson et al., 1996). A comparison

† Supported by the Max-Planck-Society and the Medical Research Council.

* Author to whom correspondence should be addressed. E-mail: geeves@mpi-dortmund.mpg.de.

‡ Max-Planck-Institut für Molekulare Physiologie.

§ Max-Planck-Institut für Medizinische Forschung and National Institute for Medical Research.

⊗ Abstract published in *Advance ACS Abstracts,* December 15, 1996.

[1] Abbreviations: ELC, essential light chain; LCBD, light chain binding domain; mantADP, 2′(3′)-*O*-(*N*-methylanthraniloyl)adenosine 5′-diphosphate; MHF, myosin head fragment; pyr-actin, pyrene-labeled actin; RLC, regulatory light chain; S1, myosin subfragment 1; ul-actin, unlabeled actin.

S0006-2960(96)02166-6 CCC: $14.00

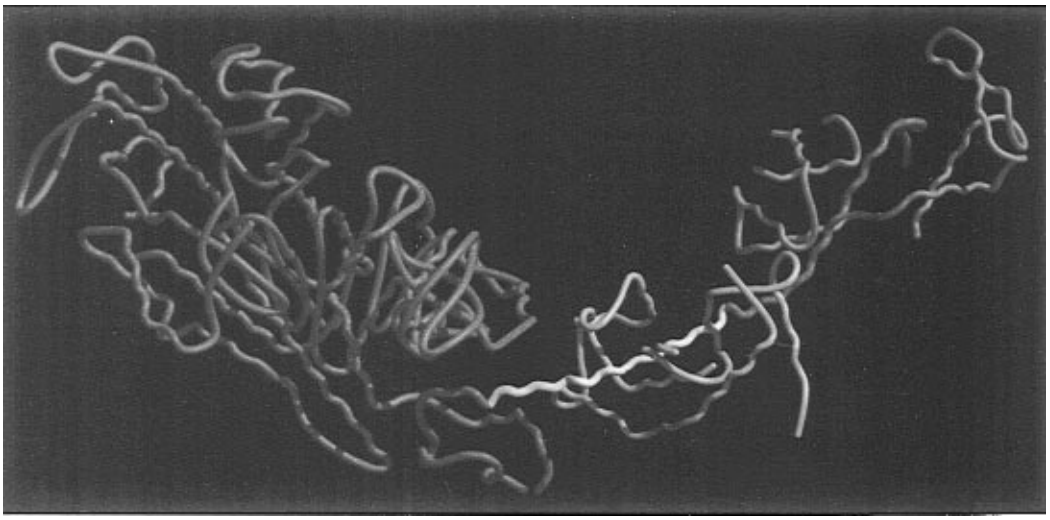

FIGURE 1: Termination sites of myosin head fragments used in this work are shown superimposed on the three-dimensional backbone structure of chicken subfragment 1 (Rayment et al., 1993). The main chain of the globular head is shown in red (*D. discoideum* aminoacids 1−754; equivalent sites in chicken are listed in Table 1), amino acids 755−761 are in green, amino acids 762−781 are in yellow, and remainder of the main chain is in red. The essential light chain is in blue and the regulatory light chain in pink.

Table 1: Termination Sites for Myosin Head Fragments[a]

motor domain	*D. discoideum*	*G. gallus*
M754	Ile-754	Leu-775
S1dC[b]	Glu-759	Asp-780
M761	Arg-761	Lys-782
MD[c]	Trp-776	Phe-797
M781	Val-781	Glu-802

[a] The C-terminal termination sites for the fragments used here and those used by Itakura et al. (1993) and Waller et al. (1995). The termination sites in the *D. discoideum* myosin heavy chain sequence and the corresponding sites in chicken skeletal myosin are listed. The following N- and C-terminal extensions were added to the above head fragments when expressed in *D. discoideum*. Residues that are not part of the native myosin sequence are underlined. M754: MDGTEDPIHD...LARILGSTRDALH$_8$. M761: MDGTEDPIHD...EEAREQRLGSTRDALH$_8$. M781: MH$_7$TED...KV. [b] S1dC: S1 catalytic domain of *D. discoideum* myosin II (Itakura et al., 1993). [c] MD: motor domain of chicken myosin produced by proetolytic digestion (Waller et al., 1995).

of the termination site of the constructs used here and in related studies is shown in Table 1.

MATERIALS AND METHODS

Protein Expression and Purification. *D. discoideum* transformants were grown at 21 °C in DD-broth 20 containing (per liter): 20 g of protease peptone L85 (Oxoid), 7 g of yeast extract (Oxoid), 8 g of glucose, 0.33 g of $Na_2HPO_4.7H_2O$, and 0.35 g of KH_2PO_4. Transformants were obtained by electroporation and continuously grown in the presence of 10 μg/mL aminoglycoside G418 (Manstein et al., 1995a). Plasmids used for transformation were derivatives of the extrachromosomal vectors pDXA-3H and pDXA-HC (Manstein et al., 1995a). The myosin−α-actinin fusion constructs were created by linking codon 754 or 761 of the *D. discoideum mhc*A gene to codon 264 of the *D. discoideum* α-actinin gene. Constructs fused to one central α-actinin repeat extended to codon 387 and those tagged with two repeats to codon 505. DNA fragments encoding one or two α-actinin repeats were obtained by PCR from a cDNA construct (Noegel et al., 1987). M754, M761, and all α-actinin fusion constructs (M754-1R, M754-2R, M761-1R, and M761-2R) carry a C-terminal affinity tag consisting of eight His residues. M781 extends to codon 781 of the *D. discoideum mhc*A gene and carries an N-terminal tag consisting of seven His residues. Transformants were screened for protein production, and the His-tagged myosin fragments were purified as described by Manstein and Hunt (1995b). Yields of up to 8 mg of each construct/L of culture medium were obtained, and SDS gels showed the presence of a single band of protein when loaded at 10 μg per lane. Thus even the M781 construct which has a partially intact binding site has no detectable light chain present. M864 was purified as described previously (Ritchie et al., 1993). Electrospray mass spectra were aquired on a VG Platform instrument with on-line trapping as described by Aitken et al. (1995).

Stopped-Flow Experiments and Fluorescence Titrations. Stopped-flow experiments were performed at 20 °C with a Hi-tech Scientific SF61 or SF-61MX stopped-flow spectrophotometer equipped with a 100 W Xe/Hg lamp and a monochromator. Pyrene fluorescence was excited at 365 nm and detected after being passed through a KV 389 nm cutoff filter. Tryptophan fluorescence, excited at 290 nm, was monitored through a WG 320 nm cutoff filter. Light scattering was collected at 90° to the incident light at 405 nm. Data were stored and analyzed using software provided by Hi-Tech. Transients shown are the average of three to five consecutive shots of the stopped-flow machine. All concentrations refer to the concentration of the reactants after being mixed in the stopped-flow observation cell. Fluorescence titrations were carried out on a SLM 8100 spectrofluorometer and a Aminco-Bowman Series 2 luminescence spectrometer at 20 °C using excitation/emission bandwidths of 4 nm. Pyrene fluorescence was excited at 365 nm with emission at 405 nm. Typical working volumes of 700 μL were used. The experimental buffer used throughout was 25 mM HEPES, 5 mM $MgCl_2$, and 100 mM KCl, pH 7.0.

Affinity of Actin for MHF. The affinities were measured using a novel stopped-flow method in which 30 nM pyractin was preincubated with different concentrations of MHF. The complex was then mixed with ATP in the stopped-flow instrument, and the amplitude of the observed transient gave

an estimate of the concentration of the acto·MHF complex present at equilibrium (Kurzawa & Geeves, 1996).

Proteins and Reagents. Rabbit actin was purified by the method of Lehrer and Kerwar (1972) and labeled with pyrene (pyr-actin) as previously described (Criddle et al., 1985). The 2′(3′)-*O*-(*N*-methylanthraniloyl) derivative of ADP (mant·ADP) was prepared by reaction with *N*-methylisatoic anhydride as described by Hiratsuka (1983), except that after reaction it was purified on a DEAE-cellulose column as described in Woodward et al. (1991).

RESULTS AND DISCUSSION

Previous studies of the full-length *Dictyostelium* myosin head (M864) have shown that the interaction of the fragment with nucleotide and actin appears to follow the same basic mechanism that was described for S1 from rabbit fast muscle myosin and other muscle myosins (Ritchie et al., 1993; Marston & Taylor, 1980). Therefore, the ATP binding and hydrolysis by the fragments have been analyzed in terms of the model shown in Scheme 1 based on that of Bagshaw et al. (1974). In this scheme M is MHF, and the asterisks refer to different conformations of the protein as detected by intrinsic protein fluorescence. Step 1 is the formation of the binary collision complex followed by an almost irreversible rapid isomerization to the M*·ATP complex. This is followed by the reversible cleavage step. In a subsequent rate-limiting step phosphate is released followed by the faster release of ADP.

Scheme 1

$$\mathrm{M} + \mathrm{ATP} \underset{k_{-1}}{\overset{k_{+1}}{\rightleftharpoons}} \mathrm{M{\cdot}ATP} \underset{k_{-2}}{\overset{k_{+2}}{\rightleftharpoons}} \mathrm{M^{*}{\cdot}ATP} \underset{k_{-3}}{\overset{k_{+3}}{\rightleftharpoons}} \mathrm{M^{**}{\cdot}ADP{\cdot}P_i}$$

The experiments in the presence of actin were analyzed in terms of models developed by Millar and Geeves (1983) and Siemankowski and White (1984) and used previously for studies of acto·S1 and acto·M864 and acto·M754 (Scheme 2). In this scheme A and M represent actin and MHF, respectively. The first step after mixing acto·MHF and ATP is the rapid equilibration between A·M and ATP defined by the equilibrium constant $\mathbf{K_1}$; this is followed by an isomerization of the ternary complex which limits the maximum rate of actin dissociation from the complex. Thus the observed rate constant for the ATP-induced dissociation of actin from the complex is defined by

Scheme 2

$$\mathrm{A{\cdot}M} + \mathrm{ATP} \overset{\mathbf{K_1}}{\rightleftharpoons} \mathrm{A{\cdot}M{\cdot}ATP} \xrightarrow{\mathbf{k_{+2}}} \mathrm{A} + \mathrm{M{\cdot}ATP}$$

$$\mathrm{A{\cdot}M{\cdot}ADP} \overset{\mathbf{K_D}}{\rightleftharpoons} \mathrm{A{\cdot}M} + \mathrm{ADP}$$

$$k_{\mathrm{obs}} = [\mathrm{ATP}]\mathbf{K_1}\mathbf{k_{+2}}/(1 + \mathbf{K_1}[\mathrm{ATP}]) \qquad (1)$$

In the presence of ADP there is competition between the two nucleotides in binding to A·M. Assuming a rapid equilibrium between A·M and the ADP-bound state, then for a fixed ATP concentration the k_{obs} is given by the equation:

$$k_{\mathrm{obs}} = k_0/(1 + [\mathrm{ADP}]/\mathbf{K_D}) \qquad (2)$$

where k_0 is the observed rate constant in the absence of ADP and $\mathbf{K_D}$ is the dissociation constant of ADP (Siemankowski & White, 1984).

In the following section we represent the results of a transient kinetic analysis in terms of the above models for M761 and M781. These are compared with data previously published for M754 (Woodward et al., 1995) and the full-length *D. discoideum* myosin head M864 (Ritchie et al., 1993). Where available, the original data for M754 and M864 are shown in the figures. Where no specific experimental data points are available in the relevant concentration range, the predicted curves are plotted on the basis of the derived rate constants.

ATP Binding to MHF. The rate of ATP binding to the actin-free head fragment was monitored from the increase in intrinsic protein fluorescence following addition of excess ATP. The observed process could be fitted to a single exponential [$F = F_0(1 - e^{-k_{\mathrm{obs}}t})$; Figure 2A], and k_{obs} was linearly dependent on ATP concentrations in the range of 5−25 μM. The second-order rate constant of binding (K_1k_{+2}) is defined by the gradient of the plot in Figure 2B, and values of K_1k_{+2} were similar for M864, M761, and M781 but slower by a factor of 10 for the shortest fragment M754 (Table 2). At higher ATP concentrations (>1 mM) k_{obs} was no longer linearly dependent upon [ATP], and the data are shown in Figure 2C with the best fit to a hyperbola ($k_{\mathrm{obs}} = k_{\mathrm{max}}[\mathrm{ATP}]/([\mathrm{ATP}] + K_{0.5})$] superimposed. The values of $k_{+3} + k_{-3}$ shown in Table 2 were obtained from the fitted value of k_{max}. This parameter shows more variability between the proteins. M864 and M781 have similar values and are 4−5-fold slower than that for M761; M754 is midway between M864 and M761. The mechanism of ATP binding and cleavage shown in Scheme 1, where ATP binding is a rapid, almost irreversible step, does not predict a hyperbolic dependence of k_{obs} upon [ATP]. $K_{0.5}$ in this case simply represents the [ATP] at which $K_1k_{+2}[\mathrm{ATP}] \approx (k_{+3} + k_{-3})/2$. Thus the large variations observed in $K_{0.5}$ reflect changes in both the rate of ATP binding (K_1k_{+2}) and ATP cleavage ($k_{+3} + k_{-3}$).

The amplitude of the fluorescence changes observed on mixing with ATP varied between the four fragments. M761 gave the largest fluorescence change (17%). The changes observed upon binding of ATP to M754, M781, and M864 were 9%, 5%, and 4%, respectively. In every case the amplitude of the fluorescence signal showed little change between 50 μM and 2 mM ATP. For rabbit myosin S1 the fluorescence change is believed to consist of two components, one associated with the binding of nucleotide and the second to the ATP hydrolysis step (see Scheme 1). For M864 the smaller fluorescence change was suggested to result from a signal change only on the hydrolysis step. The absence of a fluorescence change on ADP binding and the absence of tryptophans (W113 and W131) in the nucleotide binding site of *D. discoideum* myosin were used as supporting arguments. The equivalent residues to W113 and W131 in chicken skeletal muscle myosin are D112 and R130 in the *D. discoideum* myosin II heavy chain sequence. The larger percentage fluorescence increase in M754 was then attributed to the loss of tryptophans (W776, W808, W810, W811) in the LCBD which reduces the absolute fluorescence signal but would not affect the absolute signal change. The smaller percentage signal change in M781 could be the result of one additional tryptophan residue in the tail (W776) which would increase the absolute fluorescence relative to M754. The large fluorescence amplitude observed with M761 is

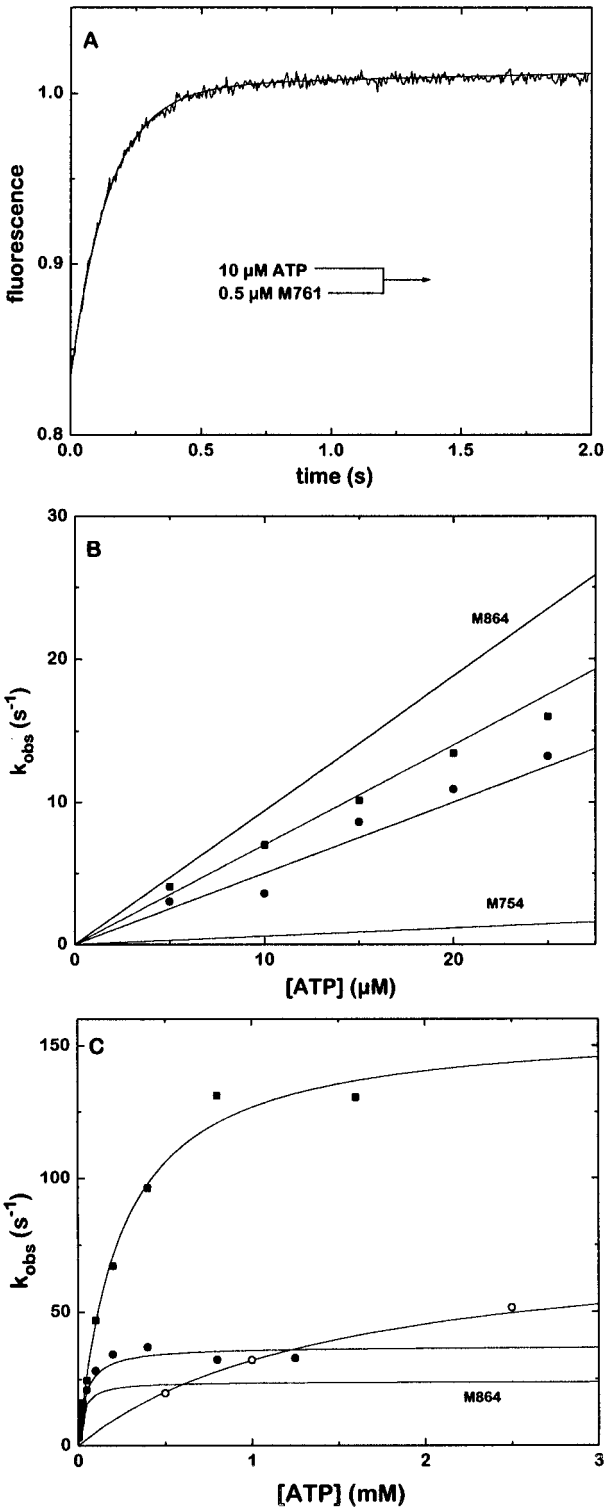

FIGURE 2: Rate of ATP binding to myosin head fragments. (A) Fluorescence change on 10 μM ATP binding to 0.5 μM M761 in the stopped-flow fluorometer. Fluorescence was excited at 295 nm and emission observed through a WG 320 filter. (B and C) Dependence of the observed rate constant of the fluorescence change on ATP concentrations of (B) 5−25 μM and (C) 0.1−3.0 mM for M761 (■) and M781(●). Data in (B) were fitted to a straight line and in (C) to a hyperbola as described in the text. The values of $K_{0.5}$ determined were 26 μM (M864), 41 μM (M781), 1433 μM (M754), and 245 μM (M761); all other values are given in Table 2. The predicted curves for M864 (no symbol) and M754 (○) based on Ritchie et al. (1993) and Woodward et al. (1995) are added to the plots. Conditions: 25 mM HEPES, 5 mM $MgCl_2$, and 100 mM KCl, pH 7.0, 20 °C.

unexpected, and an explanation may require a high-resolution structure of the MHFs.

ATP-Induced Dissociation of Acto·MHF Complexes. The binding of ATP to pyr-acto·MHF complexes was monitored by observing the exponential increase in pyrene fluorescence or the decrease in light scattering as the complex dissociates following addition of excess ATP (Figure 3A). The observed rate constants were linearly dependent upon ATP concentrations in the range of 5−25 μM as shown in Figure 3B. The second-order binding constants $\mathbf{K_1k_{+2}}$, defined by the gradient in Figure 3B, are similar for M761, M781, and M864 but 10-fold faster for M754 (Table 2). At high ATP concentrations (>2 mM) the observed rate constants saturate (Figure 3C), and the [ATP] dependence of k_{obs} could be described by a hyperbola as predicted by Scheme 2, where $k_{max} = \mathbf{k_{+2}}$ and $K_{0.5} = 1/\mathbf{K_1}$. M761 and M781 are similar to the full-length head M864 with both $\mathbf{K_1}$ and $\mathbf{k_{+2}}$ varying by less than a factor of 2. In contrast, the 10-fold faster apparent second-order rate constant of ATP binding for M754 is due to changes in both $\mathbf{k_{+2}}$ and $\mathbf{K_1}$.

Competitive Binding of ATP and ADP to Acto·MHF. The affinity of ADP for the pyr-actin·MHF was determined from the competitive inhibition of ATP-induced dissociation of pyr-acto·MHF as shown in Figure 4A. Again the exponential increase in pyrene fluorescence or the decrease in light scattering during the dissociation of the pyr-acto·MHF complex was monitored. The data for M864, M761, and M781 were fitted with eq 2 as shown in Figure 4B. Dissociation constants of approximately 100 μM were obtained for the three MHFs (see Table 2). As described previously (Woodward et al., 1995) and in contrast to the other acto·MHF complexes, pyr-acto·M754 exhibits a biphasic decrease of light scattering in the presence of ADP, and much tighter binding of ADP to acto·M754 was observed (K_D = 0.4 μM).

Actin Binding to Different Head Fragments. The rate of actin binding to the three short heads (M754, M761, and M781) was measured by following the exponential decrease in pyrene fluorescence observed on binding of excess pyr-actin to the head fragments (Figure 5A). The observed rate constants were plotted against pyr-actin concentration (Figure 5B), and all k_{obs} were linearly dependent upon actin concentration over the range studied (2.5−7.5 μM). The second-order rate constants of pyr-actin binding (k_{on}) obtained from the gradient were similar for all three fragments (see Table 2). This measurement was not made by Ritchie et al. (1993), and so no comparison is possible to the S1-like head fragment.

The affinity of M864 and M754 for actin was determined by a standard fluorescence titration of pyr-actin with the head fragments (Woodward et al., 1995; Ritchie et al., 1993). Here we used a novel stopped-flow method for M761 and M781 (essentially a fluorescence titration in the stopped-flow machine; Kurzawa & Geeves, 1996) which we believe is more accurate and gives K_d values in general 2−3-fold tighter than those determined by a standard fluorescence titration. The data shown in Table 2 are the measured values for the four fragments. Assuming that the values for M761 and M781 are 2−3-fold tighter than expected, then the affinity to pyr-actin is similar for M864 (K_d = 70 nM), 761 (11 nM), and M754 (40 nM) but significantly weaker for M781 with an affinity of 160 nM. The reasons for the weaker affinity of M781 are not apparent.

Table 2: Results of the Transient Kinetic Analysis

	rate constant[d]	M864[a]	M781	M761	M754[b]	M761-1R	M761-2R
nucleotide binding to acto·MHF	$\mathbf{K_1k_{+2}}$ (M^{-1} s^{-1})	1.4×10^5	1.56×10^5	2.1×10^5	1.5×10^6	1.2×10^5	1.25×10^5
	$\mathbf{K_1}$ (M^{-1})	330	588	667	≤1500	286	197
	$\mathbf{k_{+2}}$ (s^{-1})	450	333	411	≥800	447	467
	$\mathbf{K_D}$ (μM)	94	100	49	0.5	140	190
actin binding to MHF	$\mathbf{K_d}$ (nM)	70	160	11	40	31.7	11.8
	k_{on} (M^{-1} s^{-1})		1.0×10^6	1.3×10^6	7×10^5	0.9×10^6	1.5×10^6
nucleotide binding to MHF	K_1k_{+2} (M^{-1} s^{-1})	9.4×10^5	5.5×10^5	6.06×10^5	5.7×10^4	5.7×10^5	5.3×10^5
	$k_{+3} + k_{-3}$ (s^{-1})	24	37	160	80	29	32
in vitro motility on nitrocellulose surface[c] (nm s^{-1})		124	nd	nd	nd	107	169
in vitro motility on antibody surface[c] (μm s^{-1})		nd	nd	nd	nd	2.51	3.28

[a] All values from Ritchie et al. (1993). [b] All values from Woodward et al. (1995) except the k_{on} value, which is from this work. [c] All values from Anson et al. (1996). [d] Experimental conditions for all measurements: 25 mM HEPES, 5 mM $MgCl_2$, 100 mM KCl, pH 7.0, 20 °C.

Overall, the myosin head fragments M761 and M781 show a kinetic behavior similar to that of the S1-like fragment M864. Only the apparent rate of the hydolysis step is 5 times faster for M761, and the affinity of actin for M781 is 5 times weaker than for M864. Every other parameter is within a factor of 2 of that measured for the full-length M864. Thus the presence of the light chains and the full integrity of the distal part of the head are not essential for the interaction of the head with neither actin nor nucleotide. Furthermore, the communication between the binding sites for actin and nucleotide on the head is not affected by lack of the LCBD as shown by the similarities in the values of $\mathbf{k_{+2}}$ and the observation that the affinities of ATP and ADP are reduced to the same extent by actin in M864, M761, and M781. In addition, these studies suggest that the presence of the His tag, on either the C-terminus (M761) or the N-terminus (M781) does not have a major influence on the properties of the myosin motor.

The loss of peptide 755−761 has a dramatic effect on the kinetic properties of the head fragment as shown by the behavior of M754. The major changes in comparison with M761 are 10-fold slower binding of nucleotide to M754, 10-fold faster binding of ATP to acto·M754, and a 100-fold tighter binding of ADP to acto·M754. In our original study of M754 we suggested that the apoenzyme may be less stable than the full-length head and as a result the nucleotide binding site may not be fully formed, resulting in lower rates of nucleotide binding. Once either nucleotide or actin is bound, however, the protein is stabilized, and hence rates of ATP hydrolysis by M754 and rates of ATP binding to acto·M754 are fast. Support for this interpretation has recently been provided by differential scanning calorimetry studies of these proteins (Levitsky et al., 1997). Unfortunately, in the crystal structure of the *D. discoideum* truncated head fragment this area is not resolved, and therefore any possible direct role of this peptide in the integrity of the head structure cannot be fully assessed (Fisher et al., 1995; Smith & Rayment, 1996). However, it remains clear that the absence of this peptide does have dramatic effects on the properties of the head in both the presence and absence of actin; i.e., the affinity of ADP for acto·M754 is very high, and the presence of ADP on M754 does not have a marked affect on the affinity of actin for M754 (Woodward et al., 1995). This observation may have significance in the possible role of the LCBD in regulating the ATPase activity of myosin. It is known that the regulatory light chain can influence the ATPase activity of myosin and actomyosin through calcium binding in molluscan myosin or phosphorylation in both vertebrate and nonvertebrate myosins. Thus a communication pathway must exist between the regulatory light chain and the ATPase site on the head. The recent work of Houdusse and Cohen (1996) suggested a possible communication pathway between the regulatory light chain and the nucleotide binding site through a region they termed the converter domain (residues Asp4−Trp113 and Cys674−Lys782 of chicken S1 and Ile4−Asp113 and Cys655−Arg761 of *D. discoideum*). The change in the affinity of ADP for acto·M754 and the slow release of ADP may reflect a specific change in the interaction between 754−761 and the converter region which is communicated to the nucleotide binding site. A similar structural change could be brought about by a conformational change in the LCBD as a result of phosphorylation or Ca^{2+} binding to the regulatory light chain.

Although the two longer fragments (M761, M781) behave normally in all of the assays presented here, neither protein nor the M754 showed any signs of actin movement in a motility assay (M. Anson and D. J. Manstein, unpublished experiments). As all of the biochemical properties are normal, this lack of movement could be due to the absence of a lever arm, and if this is the case, then replacing the LCBD with an artifical lever arm should restore motility. In order to create molecular motors with motility properties similar to a native myosin but which only consist of a single polypeptide chain, M761 and M754 were fused to one or two α-actinin repeats. To study the biochemical competence of these protein constructs, we screened their functional behavior using pre-steady-state kinetics as described above. The data from these measurements are summarized in Tables 2 and 3.

The comparison between M761 and the two fusion proteins, M761, connected to one or two α-actinin repeats, M761-1R and M761-2R, shows no significant differences (Table 2) between the three proteins except that $k_{+3} + k_{-3}$ is slower for both the 1R and 2R constructs and is now similar to the full-length construct M864. Thus M761-1R and -2R are almost identical to M864 in kinetic properties. Furthermore, in a parallel study we have shown that the addition of one or two α-actinin repeats now allows these proteins to move actin at high speeds in the motility assay, indeed at speeds of the same order as the parent myosin and at speeds which are proportional to the predicted length of the artificial lever arm (Anson et al., 1996). This result is consistent with the lever arm hypothesis and the work of Uyeda et al. (1996), who showed that the *in vitro* velocity of actin over full-length myosin was proportional to the number of light chains present. The data for these constructs also suggest that the interface between the ELC and the motor

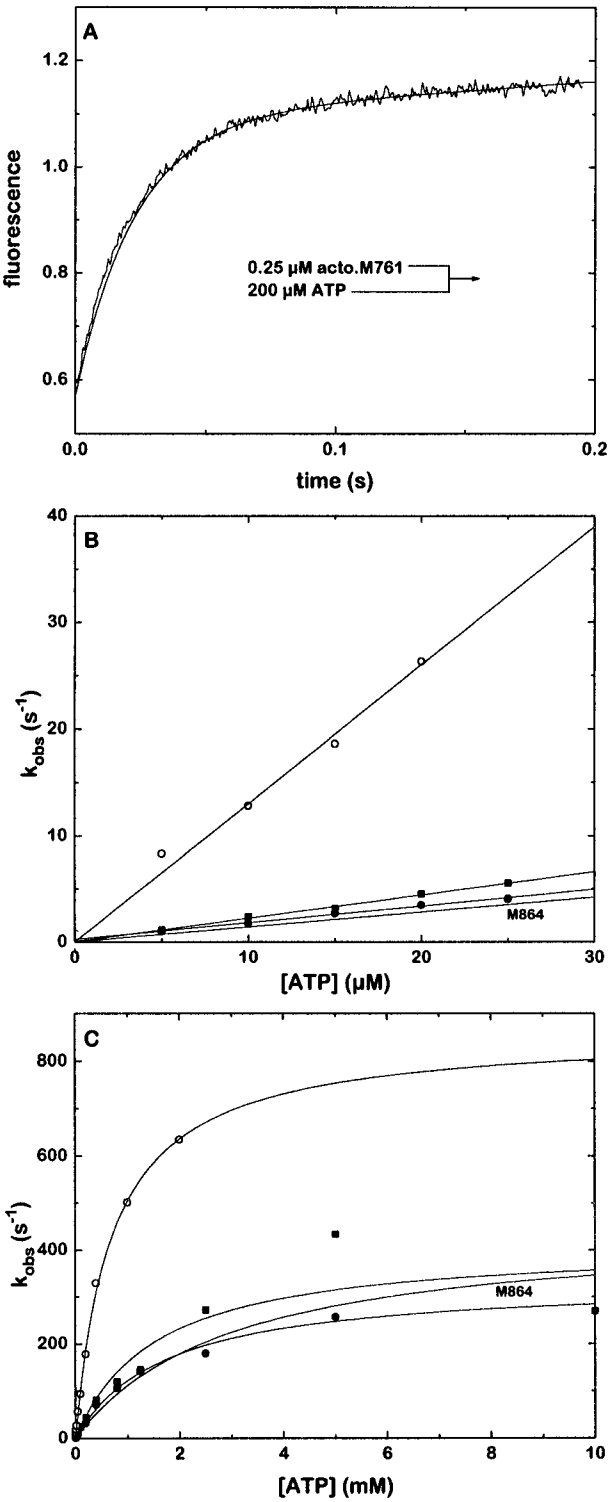

FIGURE 3: ATP-induced dissociation of the pyr-acto·MHF complexes. (A) Increase in pyrene fluorescence recorded during the dissociation of 0.25 μM pyr-acto·M761 induced by 200 μM ATP. (B and C) Plots of k_{obs} vs [ATP]. (B) The observed rate constant is linear, dependent on ATP concentrations in the range of 5−25 μM. (C) The whole data were fitted to a hyperbola. The rate constants for the isomerization step are given by the plateau values. The fitted parameters are listed in Table 2. The symbols correspond to the following *D. discoideum* myosin fragments: M761 (■), M781 (●), and M754 (○). Conditions: 25 mM HEPES, 5 mM $MgCl_2$, and 100 mM KCl, pH 7.0, 20 °C.

domain is not essential for high-veleocity actin motility. However, this interface may still be important for force generation and for the downregulation of the head by the regulatory light chain.

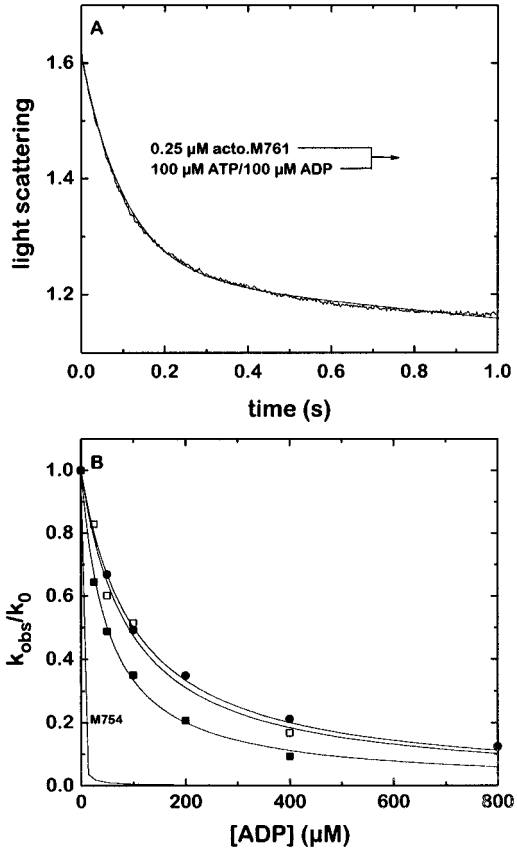

FIGURE 4: ADP inhibition of the ATP-induced dissociation of the pyr-acto·MHF complexes. (A) Light scattering signal observed during the reaction of 100 μM ATP, premixed with 100 μM ADP, with 0.25 μM pyr-acto·M761 in the stopped-flow fluorometer. (B) Plot of k_{obs}/k_0 vs ADP concentration. The dissociation constants of the ADP complexes were determined by fitting the plot to the equation $k_{obs}/k_0 = 1/(1 + [ADP]/K_D)$; k_0 = the observed rate constant in the absence of ADP (Siemankowski & White, 1984). The symbols correspond to the following *D. discoideum* myosin fragments: M761 (■), M781 (●), M864 (□).

A more resticted data set was collected for M754-1R and -2R as the major issue was whether the presence of the α-actinin repeats produces a more "normal" kinetic behavior of the head fragment. The rates of ATP-induced dissociation of the acto·MHFs were measured over the ATP concentration range 5−25 μM, and the ADP inhibition of these dissociation reactions were also measured. The results, summarized in Table 3, show that the second-order rate constants of ATP-induced dissociation of acto·MHF ($\mathbf{K_1k_{+2}}$) remained fast for all three M754 constructs. In addition, the affinity of ADP for acto·MHF remained very tight and was probably increased when the α-actinin was present as the affinity was too tight to measure directly using the method used for M754. However, the observed rate constant for ATP-induced dissociation of acto·M754-1R in the presence of saturating ADP was more than 10-fold slower for acto·M754-1R and -2R compared to acto·M754 itself. This measures the rate constant of ADP dissociation from acto·MHF·ADP ($\mathbf{k_{-D}}$; Woodward et al., 1995) and is consistent with a 10-fold tighter binding of ADP to acto·M754-1R and -2R. Repeating the same measurement with mant·ADP gave similar results, i.e., values of $\mathbf{k_{-D}}$ more than 10-fold slower for the 1R and 2R constructs although in every case the observed rate constants for mant·ADP were twice those of ADP (see Table 3). Thus these three constructs are unlikely to be able to

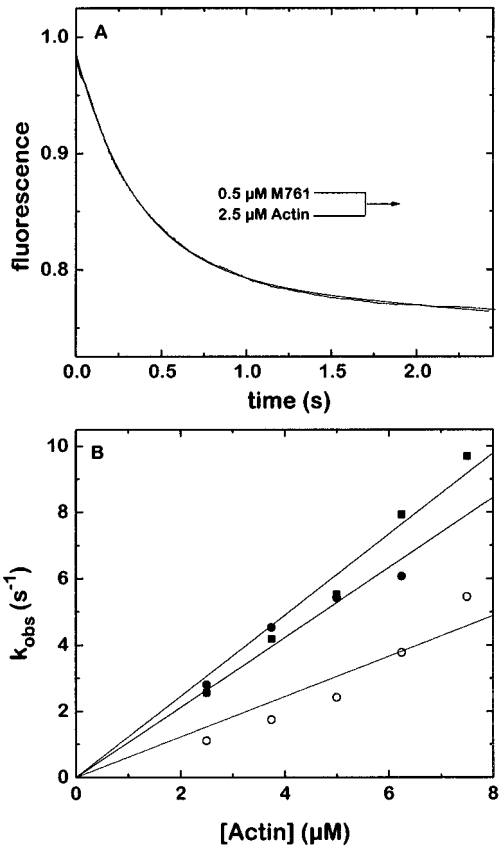

FIGURE 5: Rate of pyr-actin binding to myosin head fragments. (A) Stopped-flow record of the change of pyrene fluorescence during the binding of 2.5 μM pyr-actin to 0.5 μM M761. Pyrene fluorescence was excited at 365 nm and emission was observed through a KV 389 filter (Schott, Mainz). (B) Dependence of the observed rate constant on actin concentrations of 2.5−7.5 μM. The data are fitted to a straight line, and the parameters are listed in Table 2. The symbols correspond to the following *D. discoideum* myosin fragments: M761 (■), M781 (●), and M754 (○). Conditions: 25 mM HEPES, 5 mM $MgCl_2$, and 100 mM KCl, pH 7.0, 20 °C.

Table 3: Results

	rate constant	M754[a]	M754-1R	M754-2R
ATP	$\mathbf{K_1k_{+2}}$ (M^{-1} s^{-1})	1.5×10^6	1.1×10^6	1.0×10^6
ADP	$\mathbf{k_{-D}}$ (s^{-1})	2.3	0.17	0.14
mant·ADP	$\mathbf{k_{-D}}$ (s^{-1})	5	0.3	0.3

operate as molecular motors as the myosin head would remain tightly bound to actin with slow rate-limiting loss of ADP.

CONCLUSIONS

The kinetic properties of the catalytic domain constructs M761 and M781 show few differences from the S1-like construct M864. The fusion of one or two α-actinin repeats to the C-terminus of M761 renders the protein in kinetic terms even more similar to M864 and creates functional motor molecules which can move actin in an *in vitro* motility assay (Anson et al., 1996). This indicates that the LCBD plays no major role in defining the properties of a fully switched-on myosin head. Any regulatory function of the LCBD in this myosin must therefore be able to downregulate the myosin activity. The addition of α-actinin in place of the LCBD leaves the head in the fully switched-on state. The importance of the region between residues 754 and 761 for the function of the myosin motor was established by comparing constructs M754 and M761. Loss of the 755−761 peptide does cause a major change in the properties of the head which make it unsuitable as a molecular motor. The addition of α-actinin repeats to M754 does not alter the nucleotide binding properties of acto·M754, and it remains therefore nonfunctional as a motor (Manstein, unpublished experiments).

Their recombinant nature and the fact that they can be produced and purified in large amounts make M761, M761-1R, and M761-2R ideal constructs for systematic studies of the structure, kinetics, and function of the myosin motor.

REFERENCES

Aitken, A., Howell, S., Jones, D., Madrazo, J., & Patel, Y. (1995) *J. Biol. Chem. 270*, 5706−5709.

Anson, M. (1992) *J. Mol. Biol. 224*, 1029−1038.

Anson, M., Geeves, M. A., Kurzawa, S. E., & Manstein, D. J. (1996) *EMBO J. 15*, 6069−6074.

Bagshaw, C. R., & Trentham, D. R. (1974) *Biochem. J. 141*, 331−349.

Cohen, C., & Parry, D. A. D. (1994) *Science 263*, 488−489.

Criddle, A. H., Geeves, M. A., & Jeffries, T. A. (1985) *Biochem. J. 232*, 343−349.

Fisher, A. J., Smith, C. A., Thoden, J., Smith, R., Sutoh, K., Holden, H. M., & Rayment, I. (1995) *Biochemistry 34*, 8960−8972.

Hiratsuka, T. (1983) *Biochim. Biophys. Acta 724*, 496−508.

Houdusse, A., & Cohen, C. (1996) *Structure 4*, 21−32.

Itakura, S., Yamakawa, H., Toyoshima, Y. Y., Ishijima, A., Kojima, T., Harada, Y., Yanagida, T., Wakabayashi, T., & Sutoh, K. (1993) *Biochem. Biophys. Res. Commun. 196*, 1504−1510.

Kurzawa, S. E., & Geeves, M. A. (1996) *J. Muscle Res. Cell Motil.* (in press).

Lehrer, S. S., & Kewar, G. (1972) *Biochemistry 11*, 1211−1217.

Levitsky, D., Ponomarev, M. A., Geeves, M. A., Nikolaeva, O. P., & Manstein, D. J. (1997) *J. Muscle Res. Cell Motil.* (in press).

Manstein, D. J., & Hunt, D. M. (1995) *J. Muscle Res. Cell Motil. 16*, 325−332.

Manstein, D. J., Schuster, H.-P., Morandini, P., & Hunt, D. M. (1995) *Gene 162*, 129−134.

Marston, S. B., & Taylor, E. W. (1980) *J. Mol. Biol. 139*, 573−600.

Millar, N. C., & Geeves, M. A. (1983) *Febs Lett. 160*, 141−148.

Noegel, A., Witke, W., & Schleicher, M. (1987) *FEBS Lett. 221*, 391−396.

Rayment, I., Holden, H. M., Whittaker, M., Yohn, C. B., Lorenz, M., Holmes, K. C., & Milligan, R. A. (1993) *Science 261*, 58−65.

Ritchie, M. D., Geeves, M. A., Woodward, S. K. A., & Manstein, D. J. (1993) *Proc. Natl. Acad. Sci. U.S.A. 90*, 8619−8623.

Siemankowski, R. F., & White, H. D. (1984) *J. Biol. Chem. 259*, 5045−5053.

Smith, C. A., & Rayment, I. (1996) *Biochemistry 35*, 5404−5417.

Uyeda, T. Q. P., Abramson, P. D., & Spudich, J. A. (1996) *Proc. Natl. Acad. Sci. U.S.A. 93*, 4459−4464.

Waller, G. S., Ouyang, G., Swafford, J., Vibert, P., & Lowey, S. (1995) *J. Biol. Chem. 270*, 15348−15352.

Woodward, S. K. A., Eccleston, J. F., & Geeves, M. A. (1991) *Biochemistry 30*, 422−430.

Woodward, S. K. A., Geeves, M. A., & Manstein, D. J. (1995) *Biochemistry 34*, 16056−16064.

Yan, Y., Winograd, E., Viel, A., Cronin, T., Harrison, S. C., & Branton, D. (1993) *Science 262*, 2027−2030.

BI962166B